Journal of Applied Science and Environmental Studies
JASES
http://revues.imist.ma/index.php?journal=jases

INVESTIGATING THE CORROSION INHIBITION POTENTIALS OF *STRICHNOS SPINOSA L.* EXTRACT ON ALUMINIUM IN 0.3M HYDROCHLORIC ACID SOLUTION

A. M. AYUBA[1*], A. ABDULLATEEF[1]

[1]*Department of Pure and Industrial Chemistry, Faculty of Physical Sciences, Bayero University, Kano, Nigeria*

Received 28 Dec 2020; Revised 20 Jan 2021, Accepted 25 Jan 2021

Keywords
FTIR
SEM
Linear Polarization
Weight loss
Physisorption
Freundlich

Abstract

The corrosion inhibition potentials of *Strichnos spinosa L.* extract was assessed using weight-loss, linear polarization resistance (LPR), SEM and Fourier transform infrared spectroscopy (FTIR) methods. Influence of extract concentrations (0.2g/l to 0.6g/l) and temperatures (303K to 323K) on corrosion and corrosion inhibition of aluminium was assessed. The results showed that increase in concentration of the extract of *Strichnos spinosa L.* decreased the corrosion rate of aluminium in the hydrochloric acid media. The decrease in inhibition efficiency with increase in temperature, suggested physical adsorption of the *Strichnos spinosa L* extract on the aluminium surfaces. The kinetic and thermodynamic parameters calculated revealed that activation energy (E_a) for aluminium corrosion in hydrochloric acid solution increased in the presence of the plant extract and the values were found to be less than 80kJmol^{-1} proposing physisorption mechanism. Positive values of adsorption enthalpy, negative values of activation entropy and negative values of free energy show that the process is feasible and spontaneous. Linear polarization resistance curve shows that *Strichnos spinosa L.* extract inhibited both cathodic and anodic sites serving a mixed type inhibitor. FTIR results also showed that the inhibition mechanism was a physical type of adsorption process through the functional groups present in the extract by slight shift in absorption bands between the plant extract and that of the inhibited metal surfaces. Surface morphology also revealed that corrosion product confirmed the protection offered by the extract on the surface of the metal immersed in the acid media. The data obtained fitted well the Freundlich isotherm in relation to Langmuir isotherm tested.

1. Introduction

Corrosion is a natural process, which converts a refined metal to a more stable form, such as its oxide or hydroxide. It is the gradual destruction of materials (usually metals) by chemical reaction with their environment. Corrosion can also occur in materials other than metals, such as ceramics or polymers, although in this context, the term degradation is more common [1]. Aluminium is an important metal in many industries owing to its many excellent characteristics especially its good electrical and thermal conductivities, low density high ductility, low cost and availability for the fabrication and construction industries. It is widely used as a material for automobiles, aviation, house hold appliances, containers, electronic devices, good corrosion resistance [2]. Naturally, corrosion happens on all types of material but it had been most commonly associated with metals. Metals corrode because we use them in environments where they are chemically unstable. There are many ways/methods in which corrosion process can be controlled ie chromates were once used as corrosion inhibitors. However, environmental scientists discourage its usage due to it toxicity. In order to overcome the challenges posed by toxic inhibitors, there is need to focus future research on the use of eco-friendly corrosion inhibitors. Therefore, researchers have successfully used different plant extracts as corrosion inhibitors [3][4][5][6][7][8][9][10][11][12].

Plant extracts are obtained from materials naturally occurring substance, which are cheap and are readily available in our immediate environment as waste product that cause environmental pollution. Extracts of plant materials contain many active principles and therefore contain polar atoms such as S, N, O, P etc. due to the lone pair of electrons present on these atoms which is adsorbed on to the metal surface; loss of electrons from the metal surface can be avoided. Thus, corrosion inhibition takes place by adsorption of inhibitor molecules on metal surface, protective film is formed and corrosion is controlled [13][14][15][16].

Therefore, the present study attempted to explore the possibility of using *Strichnos spinosa L.* plant extract for the inhibition of the corrosion of aluminium in HCl solution**.** Various concentrations of the extract was used to prevent aluminium metal immersed in various hydrochloric acid media at different temperatures in presence and absence of the plant extract. Methods including weight loss, Linear polarization resistance studies were employed to evaluate corrosion rate, surface coverage and inhibition efficiencies of inhibitor. Surface characterization of the free and corroded aluminium metal shall be conducted using scanning electron microscopy (SEM) while the adsorption bands of the plant extract and the corroded metal (containing the extract) were analyzed using Fourier transform infrared (FT-IR) spectroscopy.

2. Experimantal Details

2.1 Materials

2.1.1 Collection, preparation and extraction of the plant samples

Sample leaves of *Strichnos spinosa* were collected in Kumbotso Local Government, Kano State, Nigeria and identified at the Department of Plant Biology, Bayero University Kano. A herbarium Accession number BUKHAN 0127 was assigned for reference.
The leaves were rinsed with distilled water, air dried under shade, ground to powder, sieved and 500g of the powdered were soaked in 2 L of 95% ethanol solution for two weeks. The soaked samples were filtered using Whatmann No 1 filter paper. The filtrate sample was concentrated to a thick syrup using a rotavapor (model: Recirculating chiller-F105). The thick syrup was allowed to dry by expelling the excess ethanol. The dried extract obtained was used in preparing different concentrations of the inhibitor by dissolving 0.2, 0.4 and 0.6g of the extracts in 1L 0.3M HCl solution [17-18].

2.1.2 Preparation and treatment of aluminium coupon

Aluminium sheet was the material used for the study and its composition was determined by Mini pal, a compact energy dispersive X-ray fluorescence spectrometer and the following composition was recorded: (wt %) Al(98.70), Si(0.48), Cl(0.014), K(0.04), Ca(0.01), Ti(0.005), V(0.016), Mn(0.012), Fe(0.50), Ni(0.013), Cu(0.048), Ga(0.013), In(0.10), Te(0.010), Ba(0.009), Os(0.032), Ir(0.03). This material was mechanically press-cut into different coupons, each of dimensions 3 x 2 x 0.12mm for weight loss investigation and 1cm x1cm for electrochemical study. The coupons were wet polished with different grades of SiC abrasive paper (#400 to #1200), degreased by washing with ethanol, cleaned with acetone and allowed to dry in air before preservation in a desiccator.

2.1.3 Preparation of solutions

All reagents used for this study were of Analar grade and double distilled water was used for their preparation. Acid solution of 0.3MHCl was used for weight loss and polarization studies after they had been standardized, while the concentration range for the plant extract was 0.2g/L, 0.4g/L and 0.6g/L respectively.

2.2 Experimental Methods

2.2.1 Weight loss measurements

All the weighing of the aluminium specimens, before and after immersion, was done using analytical weighing balance. A previously weighed metal (aluminium) coupon was completely immersed in 100 ml of the various test solutions of 0.0, 0.2, 0.4 and 0.6g/L prepared in 0.3HCl concentration in open beakers. The beakers were covered with polyethene, banded with rubber band and inserted into a water bath maintained differently at temperatures of 303, 313 and 323K. After every one hour the corrosion product was removed (withdrawn from the test solution), washed with distilled water then ethanol for a total period of four hours. The washed coupon was rinsed in acetone and air dried before re-weighing. From the change in the weights of the specimens, the corrosion rates (CR), the degree of surface coverage (θ) and inhibition efficiency (%I.E) of the inhibited and uninhibited systems were calculated using the following equations 1, 2 and 3 [1-7].

$$CR = \frac{\Delta W}{At} \quad (1)$$

$$\theta = \frac{\%\, I.E}{100} \quad (2)$$

$$\%\, I.E = \frac{W_f - W_i}{W_f}\, x\, 100 \quad (3)$$

Where W_f and W_i are the weight losses (g) for alumimium coupon in the absence and presence of the inhibitor respectively, θ is the degree of surface coverage of the inhibitor, $\Delta W = W_f - W_i$, A is the area of the aluminium coupon (cm^2), t is the period of immersion (hours) and CR is the change in weight loss of aluminium with time, t.

2.2.2 Linear polarization resistance measurement

Aluminium coupons were mechanically press-cut into a dimension of 1cm x1cm for investigation during the Linear polarization resistance studies. The coupons were wet polished with different grades of SiC abrasive paper (#400 to #1200), degreased by washing with ethanol, cleaned with acetone and allowed to dry in the air before preservation in a desiccator. The linear polarization was carried out in an acid solution of 0.3M (HCl) and at 30^{o}C, while the concentration range for the inhibitors was 0.2g/L,0.4g/L and 0.6g/L respectively.

Linear Polarization Resistance measurements were performed using a Princepton Applied Research VersaSTAT4 which employed a three-electrode cell, namely a platinum counter

electrode (CE), saturated calomel with Ag/AgCl reference electrode (RE) and aluminium working electrode (WE). Prior to all electrochemical measurements, a 30 min period was allowed as a period of stabilization, since it was proved to be an appropriate period to attain a stable value of E_{corr}. Tafel curves were measured at the potential range of -250 to +250 mV (SCE) and scan rate of 1 $mV.s^{-1}$.

Linear polarization resistance (LPR) plots and the slope of the plots in the vicinity of the corrosion potential gave the polarization resistance (Rp). The inhibition efficiency (IE%) was calculated using equation 4:

$$\%I.E = \frac{R_{p(inh)} - R_{p(inh)}}{R_{punh}} \times 100 \qquad (4)$$

Where, $Rp_{(inh)}$ and $Rp_{(inh)}$ are the uninhibited and inhibited polarization resistance, respectively [19-24]

2.2.3 Fourier transform infrared (FT-IR) analysis

FTIR Instrument of model: Cary 630 FTIR Spectrophotometer (Agilent Technologies) was used to identify the major functional groups present in leaves extract of *Strichnos spinosa*, corroded aluminium sample, and corrosion product of inhibited aluminium metal in HCl solution.

Each coupon was separately dipped in 100 mL of 0.3 M (HCl) of acid-inhibitor concentration respectively for 4 hours to form an adsorbed layer after which they were removed, dried and scraped with a sharp razor blade and the analysed. The samples analysis was done by scanning the sample through a wave number range of 650-4000 cm^{-1}[25-27].

2.2.4 Scanning electron microscopy (SEM) analysis

The surface morphological change of aluminium coupon sample was investigated using Scanning Electron Microscope (Phenom World Eindhoven). Scanned micrographs of the aluminium coupons before and after different concentrations of *Strichnos spinosa L.* extract adsorption in 0.3M HCl were taken at an accelerating voltage of 15.00 kV and x1500 magnification.

3. Results and Discussion

3.1 Weight Loss Measurements

Rate of corrosion ($gh^{-1}cm^{-2}$) and inhibition efficiency (% I. E.) of aluminium exposed to 0.3MHCl at different concentrations of *Strichnos spinosa L.* extract are shown in Table 1. It is experiential that corrosion rate for the aluminium coupon specimen was found to be decreased with the consecutive enhancement in inhibition effectiveness on increasing *Strichnos spinosa L* extract concentration from 79.155% to 98.041%. This performance could be due to the increase in the adsorption of *Strichnos spinosa L* extract at the metal/electrolyte boundary on increasing its concentration. This inference established that *Strichnos spinosa L* extract acts as an efficient corrosion inhibitor.

Table 1: Surface coverage, Inhibition Efficiencies of *Strichnos spinosa L* and Corrosion Rate of Aluminium and in 0.3MHCl at varying temperatures

Temperature	System	Surface Coverage (θ)	Inhibition Efficiency (%IE)	Corrosion rate ($gh^{-1}cm^{-2}$)
303K	0.0g/L	-	-	0.0803
	0.2g/L	9560.3	95.603	0.0751
	0.4g/L	9620.9	96.209	0.0680
	0.6g/L	9804.1	98.041	0.0596
313K	0.0g/L	-	-	0.0856
	0.2g/L	8200.3	82.003	0.0796
	0.4g/L	8299.4	82.994	0.0726
	0.6g/L	8526.0	85.26	0.0650
323K	0.0g/L	-	-	0.0944
	0.2gL	7915.5	79.155	0.0803
	0.4g/L	8085.5	80.855	0.0751
	0.6g/L	8471.5	84.715	0.0700

3.2 Linear Polarization Resistance Measurements

Linear polarization resistance curves for aluminium metal in 0.3 M HCl solutions in the absence and presence of different concentrations (0.0g/l, 0.2g/l, 0.4g/l and 0.6g/l) of *Strichnos spinosa L* are shown in Figure 1. From the plots, it can be observed that the cathodic and anodic branches of the polarization curves are shifted towards lower currents to similar extent in presence *Strichnos spinosa L*, which may be as a result of the blocking effect of the adsorbed inhibitor molecules. It can also be deduced from the curves that the studied extract inhibits corrosion by controlling both anodic and cathodic reactions (i.e. mixed-type inhibitor) since both the anodic and cathodic reactions are affected by the *Strichnos spinosa L* extract. This implies that the addition of the extract reduces the anodic dissolution of aluminium and also retards the cathodic reaction. Electrochemical parameters deduced from the polarization curves including are presented in Table 2. It can been seen that the values of anodic and cathodic Tafel slopes (β_a and β_c) obtained were found to be approximately constant and varies slightly with inhibitor concentration indicating that this inhibitor act by simply blocking the available surface area on the aluminium coupon [28]. Also values of the inhibition efficiencies presented in Table 2 for various *Strichnos spinosa L.* extract concentrations showed a high efficiency with increasing extract concentration. Comparing the inhibition efficiencies obtained from weight loss method as reported in table 1 and that of linear polarization reported in Table 2, a clear correlation was established between both but with that of weight loss been higher.

Table 2: Linear Polarization Resistant Data for *Strichnos spinosa L*. in 0.3MHCl Medium

Syste	E_{corr}(mV	$I_{corr}(\mu A)$	β_c(m	β_a(mV	C.R(mmp	I.E(%
Blank	-701.151	-389.197	102.27	29.996	4.2362	-
0.2g/L	-732.735	-70.166	82.463	64.026	0.76373	81.97
0.4g/L	-751.259	-57.723	71.453	59.755	0.6283	85.17
0.6g/L	-735.776	-44.827	44.45	45.226	0.48793	88.48

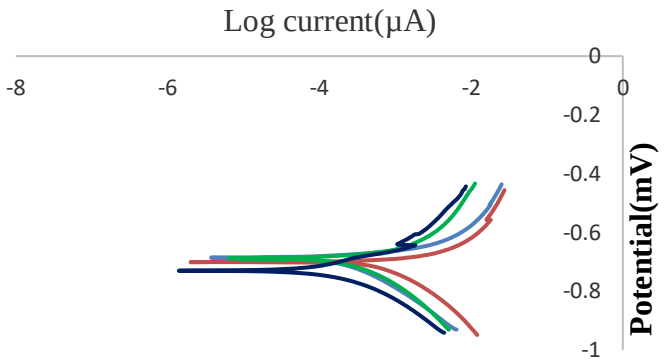

Figure 1: Linear polarization resistance curves for Al in 0.3 M HCl solution without and with various concentrations of the extract (Red = blank, blue= 0.2g/L, Green= 0.4g/L, Purple = 0.6g/L) compound at 303K

3.3 Fourier Transform Infrared (FTIR) Spectrometry

The functional groups present within the adsorption film that resulted during the adsorption process were investigated using FTIR technique. The FTIR spectra of the studied *Strichnos spinosa L* extract and aluminium surfaces after corrosion in the presence and absence of *Strichnos spinosa L* are shown in Figure 2 (a-c). From Figure 2a which is that of the corroded metal without the *Strichnos spinosa L* extract, it can be observed that the sample is almost FT-IR inactive with some weak peaks showing which may be due to impurities either on the aluminium metal surface or in the 0.3M HCl solution used for the corrosion process.

The FTIR spectrum of *Strichnos spinosa L* extract (Figure 2b) and that of the aluminium metal corrosion product in *Strichnos spinosa L* extract (Figure 2c), showed that most of the peaks for the extract were also noticed in the surface films of the inhibitor on the metal surface, suggesting that most of the functional groups within the extract was also present in the surface film. Even though some of these peaks have shown some significant shift in wave numbers, this may be due to the weak associative interactions between the extract and the metal surface. This further confirms the fact that the extract was actually adsorbed on the metal surfaces through the mechanism of physical adsorption.

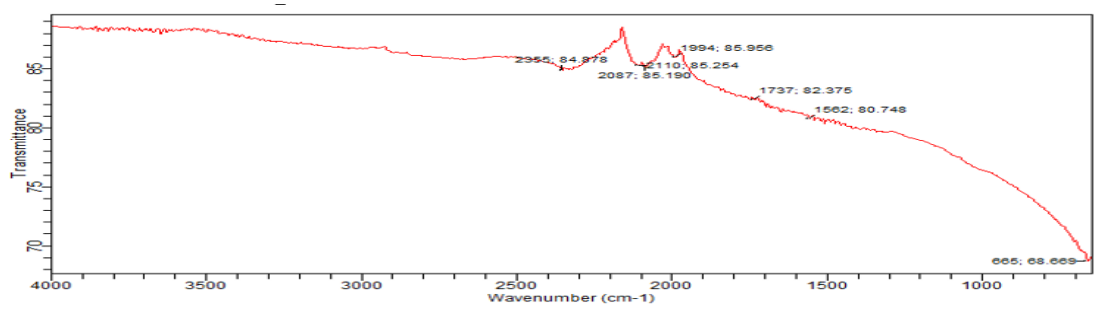

Fig. 2a: FTIR Spectrum of corrosion product of aluminium immersed in blank HCl

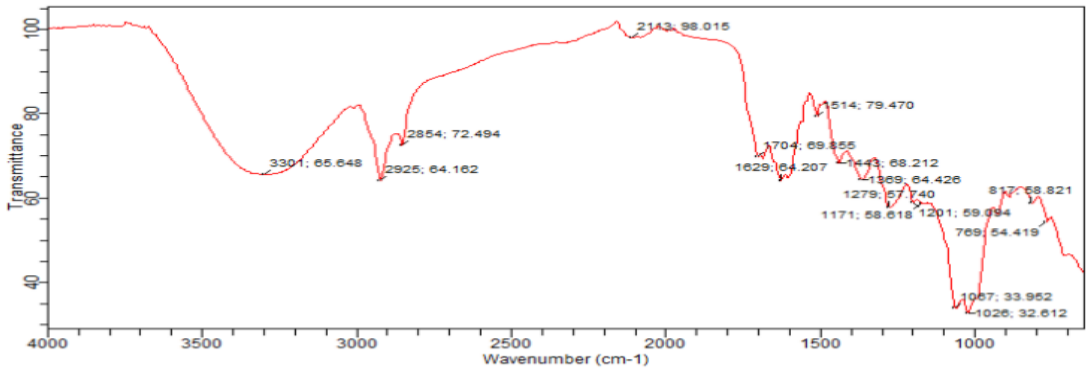

Fig. 2b: FTIR Spectrum of the leaves extract of *Strichnos spinosa L*

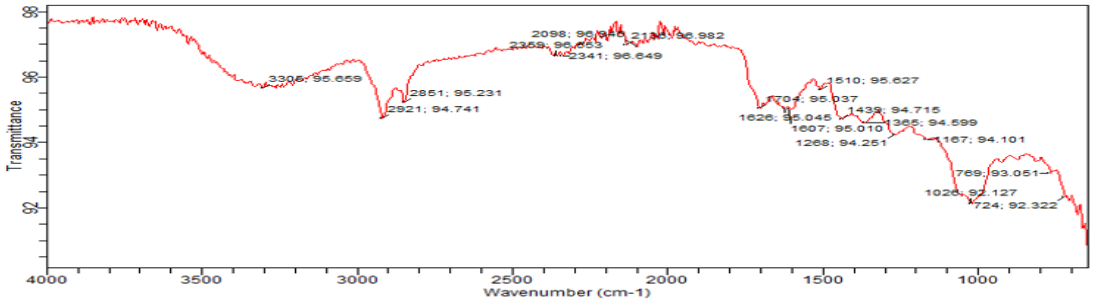

Fig. 2: FTIR Spectrum of the corrosion product of aluminium immersed in inhibited HCl

3.4 Scanning Electron Microscopy (SEM)

SEM images of aluminium before and after corrosion in different concentrations of the *Strichnos spinosa L* extract in 0.3M HCl is as shown in Figures 3(a-d). According to SEM micrographs observed, the surfaces of blank uninhibited corroded aluminium in 0.3M HCl and that of the same metal in different concentrations of *Strichnos spinosa L extract* are quite different from each other. This is an indication that the plant extract was adsorbed onto the surface of the aluminium metal. The surface of aluminium in the blank solution containing 0.3M HCl show lots of rough surfaces, pores, cracks and patches which can be seen to gradually disappear as the concentration of the *Strichnos spinosa L* extract increases from 0.2g/L to 0.6g/L in 0.3M HCl. This proves that the *Strichnos spinosa L* extract is an adsorption inhibitor.

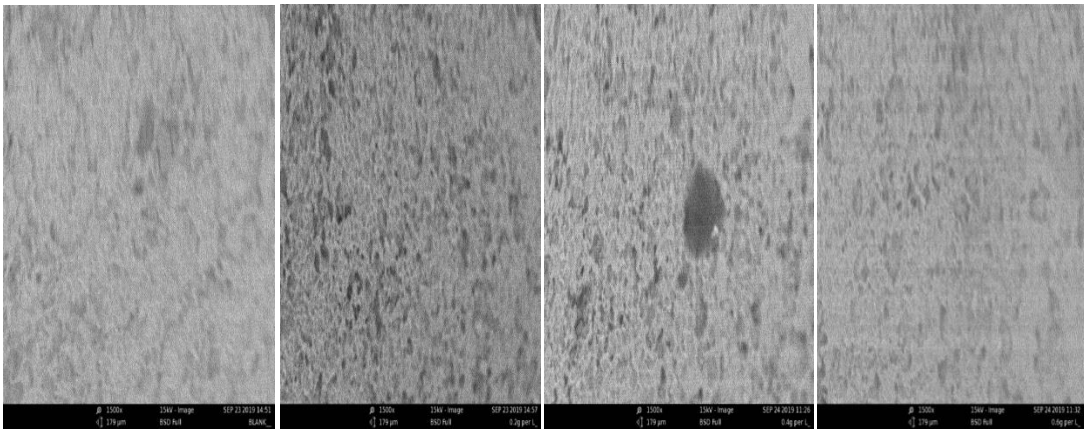

(a) **(b)** **(c)** **(d)**

Fig. 3. SEM micrographs for aluminium in a) 0.3MHCl – blank, b) 0.2g/L, c) 0.4g/L, d) 0.6g/L extract

3.5 Adsorption Isotherm Studies

Adsorption isotherms (Langmuir and Freundlich) were employed to predict the mechanism interaction between inhibitor and the surface of aluminium substrates. In this study, results

obtained for the degree of surface coverage (Θ) at all temperatures were fitted into different adsorption isotherms. Figure 4 shows the Freundlich adsorption isotherm for *Strichnos spinosa L*. extract with linear correlation coefficient, R^2 values closer to unity and was used to define the type of adsorption process. The values of K_{ads} obtained from the intercept were used to calculate the standard free energy (ΔG_{ads}) via using equation 5:

$$\Delta G_{ads} = -RTIn(K_{ads}55.5) \quad (5)$$

Where R is the molar gas constant, T is the absolute temperature and 55.5 is the concentration of water in solution expressed in M.

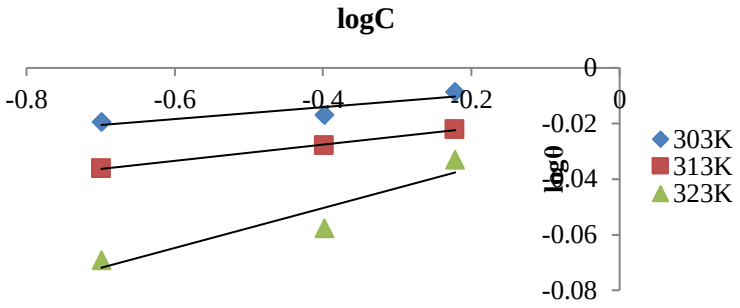

Fig. 4: Freundlich isotherm for *Strichnos spinosa L* on aluminium surface in 0.3MHCl solution at various temperatures

Table 3: Adsorption isotherms parameters for *Strichnos spinosa L* in 0.3 M HCl

Isotherms	Temp(K)	Slope	R^2	K_{ads}	ΔG_{ads}(kJmol^{-1})
Langmuir	303	0.397	0.570	0.212	-6.211
	313	0.220	0.556	0.420	-8.196
	323	0.121	0.555	0.618	-9.495
Freundlich	303	0.021	0.826	0.989	-10.092
	313	0.029	0.997	0.966	-10.363
	323	0.071	0.876	0.953	-10.695

From table 3, the calculated values of standard free energy of adsorption process were negative for all methods used and ranged from −6.211 to −10.695 kJ mol^{-1} for *Strichnos spinosa L* extract. The negative value of ΔG_{ads} indicates that the adsorption of inhibitor on the aluminium surface substrates occurs spontaneously. Usually, values of standard free energy values lesser or closer to −20 kJ mol^{-1} are reliable with electric charges between molecules inhibitor and surface charged steel substrate (physisorption) while those more negative than –40 kJ mol^{-1} involves sharing of electrons from the inhibitor molecules to the metal surface to form a chemical bonding (chemisorptions) [26–28]. In the case of *Strichnos spinosa L* extract, ΔG_{ads} value of the inhibitor was found to be from −6.211 to −10.695 kJ mol^{-1}, this indicates the phenomena of adsorption of inhibitor on the metal surface by physical adsorption process.

3.6 Effect of Temperature

The effects of temperature on the corrosion rate and inhibition efficiency enhance the calculation of kinetic and thermodynamic parameters for the inhibition and the adsorption processes. These parameters are useful in interpreting the nature/type of adsorption occurring between the inhibitor and the metal surface. The result reported in Table 1 shows that inhibition efficiency of *Strichnos*

spinosa L extract decreased with increase in temperature. The value of activation energy (Ea) was calculated using the Arrhenius law equations 6 [5, 7, 22]:

$$\frac{lnCR}{T} = lnA - Ea/RT \qquad (6)$$

Where A is a constant which depends on the metal type, R is the universal gas constant, and T is the absolute temperature. The plot of ln(CR/T) versus reciprocal of absolute temperature (1/T) gave a straight line with slope = $-E_a/R$, from which the activation energy values for the corrosion process was calculated. The Arrhenius plot for the corrosion of aluminium metal in 0.3MHCl acid in the absence and in the presence of different concentrations of inhibitor is shown in Fig. 5

$$\frac{lnCR}{T} = ln({}^{R}/_{N_A h} + {}^{\Delta S_a}/_{RT}) - \Delta Ha/RT \qquad (7)$$

The plot of ln(CR/T) versus reciprocal of absolute temperature (1/T) from equation 7, as shown in Figure 6 gave a straight line with slope = $-\Delta H_a/R$, and intercept of $ln({}^{R}/_{N_A h} + {}^{\Delta S_a}/_{RT})$ from which the activation enthalpy energy and entropy values changes for the corrosion process was calculated. The values of E_a, ΔH_a and ΔS_a are represented in table 4.

The addition of inhibitor increased the energy of activation value (E_a). This change may be attributed to the change in the mechanism of the corrosion process through physical adsorption in the presence of inhibitor molecules [24]. The energy of activation (E_a) values in the presence of the *Strichnos spinosa L* extract increased drastically with the adsorption of components of *Strichnos spinosa L* extract on the aluminium surface of the metal [24- 25]. Negative values of entropies show that the activated complex in the rate determining step is an association rather than dissociation step meaning that a decrease in disordering takes place on going from reactants to the activated complex [30].

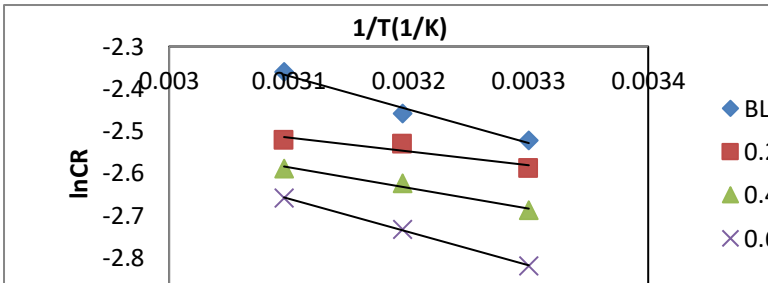

Fig. 5. Arrhenius plots for the corrosion of Al in 0.3 M HCl at different concentrations of *Strichnos spinosa L* extract**.**

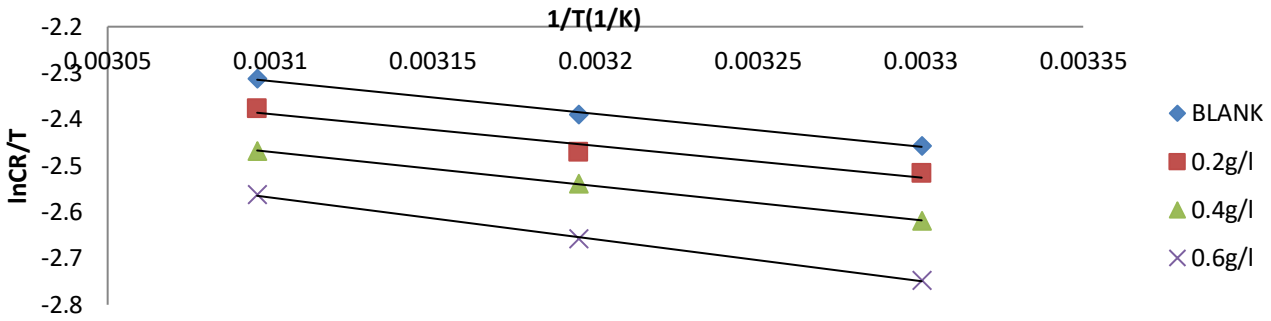

Fig. 6. Variation of natural log (Corrosion Rate) of Aluminium with Inverse Temperature in 0.3 M HCl Containing Various Concentration of *Strichnos spinosa L* extract.

Table 4: Thermodynamic Parameters for dissolution of aluminium metal in 0.3M HCl in the absence and present of different concentrations of *Strichnos spinosa L*.

Concentraion (g/L)	E_a(kJ/mol)	ΔH_a(kJ/mol)	ΔS_a(kJ/mol)
Blank	44.94	42.40	-0.168
0.2	62.61	53.19	-0.150
0.4	65.37	50.39	-0.155
0.6	67.96	49.58	-0.159

Conclusion

The corrosion inhibition and adsorption studies of *Strichnos spinosa L* extract on aluminium surface in 0.3M HCl was examined. The outcome shows the following:

- The corrosion rate decreases and inhibition efficiency increases of the aluminium coupon in 0.3M HCl with an increase in concentration of *Strichnos spinosa L* extract. Maximum inhibition efficiency of the plant extract was achieved to be 98.041% for weight loss method and 88.48% for linear polarization resistance method at 303K.
- The linear polarization resistance studies showed that *Strichnos spinosa L*. extract performed as a mixed type of inhibitor on aluminium metal surface.
- The adsorption process followed the Freundlich isotherm model. The negative value of ΔGads, FTIR and SEM results predicted the adsorption process to be spontaneous and proceeds through physisorptions.

Acknowledgements

The authors wish to acknowledge the contributions of the Department of Pure and Industrial Chemistry, Bayero University Kano, Nigeria, for providing the chemical/reagents/instruments needed for this research.

References

1. F. Matjaz, J. Jennifer, Application of corrosion inhibitors for steels in acidic media for the oil and gas industry: a review, **Corros Sci**. 86 (2014) 17–41.
2. E. E. El-Katori and Y. M. Al Angari, Electrochemical and theoretical evaluation on the corrosion inhibition of carbon steel by organic selenides in acidic medium, **Int. J. Electrochem. Sci**.13 (2018) 4319 – 4337.
3. S. Umoren, U. Eduok, M. Solomon, A. Udoh,Corrosion inhibition by leaves and stem extracts of sidaacuta for mildsteel in $1MH_2SO_4$ solutions investigated by chemical and spectroscopic techniques, **Arab. J. Chem**. 9 (2016) 209–224..
4. K. Ramya, N. Muralimohan, Study on corrosion inhibitor in mild steel by various habitual plant extract review, **Int. J. Chem. Concepts**, 2 (2016) 70–75.
5. A. Singh, Cassia tora leaves extract as mild steel corrosion inhibitor in sulphuric acid solution, **Imperial J. Interdisciplinary Res**. 2 (2016) 698–701.
6. O. O. Dominic, O. Monday, Optimization of the inhibition efficiency of Mango extract as corrosion inhibitor of mildsteel in 1.0M H_2SO_4 using response surface methodology, **J. Chem.Technol. Metall**. 51 (2016) 302–314.
7. M. J. Meften, N. Z. Rajab. M. T. Finjan, Synthesis of new heterocyclic compound used as corrosion inhibitor for crude oil pipelines, **Am. Sci. Res. J. Eng. Technol. Sci**. 27(2017) 419–437.
8. O. U. Abakedi, V. F. Ekpo. E. E. John, Corrosion inhibition of mildsteel by Stachytarpheta indica leaf extract in acid medium, **Pharm. Chem. J.** 3(2016) 165–171.
9. T. Ramde, S. Rossi, Inhibition of the Cu65/Zn35 brass corrosion by natural extract of Camellia sinensis, **Applied Surface Science**, 307(2014) 209-216.
10. F. Suedile, F. Robert, C. Roos, M. Lebrini, Corrosion inhibition of zinc by Mansoaalliacea plant extract in sodium chloride media: Extraction, Characterization and Electrochemical Studies, **Electrochimica Acta**, 133(2014) 631-638.
11. J. Zhang, Q. Zhang, G. Chen, J. R. Zhao, D. Y. Tang, Modification of punicagranatumLinne husk extract as eco-friendly corrosion inhibitors in oil fields, **Applied Mechanics and Materials**, 488(2014) 273-276.
12. M. Dekmouche, M. Saidi, M. Hadjadj, Z. Ghiaba, M. Yousfi, Green approach to corrosion inhibition by ethyl acetate extract from Pistaciaatlantica gals in hydrochloric acid solution, **International Journal of Electrochemical Science**, 9(7)(2014) 3969-3978.
13. S. Fabienne, R. Florent, R. Christophe, Corrosion inhibition of zinc by Mansoa alliacea plant extract in sodium chloride media: extraction, Characterization and Electrochemical Studies, **Electrochim Acta**, 133(2014) 631–638.
14. L. Bammou, M. Belkhaouda, R. Salghi, Corrosion inhibition of steel in sulfuric acidic solution by the chenopodium ambrosioides extracts, **J Association of Arab for Basic and App Sci**, 16(2014) 83–90.
15. K. K. Anupama, K. Ramya, K. M. Shainy, Adsorption and electrochemical studies of Pimenta dioica leaf extracts, as corrosion inhibitor for mild steel in hydrochloric acid, **Mater Chem Phys**. 167 (2015) 28–41.

16. E. H. Naoual, F. Rabiaa, T. Mustapha, Alkaloids extract of Retama monosperma (L.) Boiss. seeds used as novel eco-friendly inhibitor for carbon steel corrosion in 1 M HCl solution: electrochemical and surface studies, **Appl Surf Sci**, 357 (2015) 1294–1305.
17. A. K. Singh, S. Mohapatra, B. Pani, Corrosion inhibition effect of Aloe Vera gel: gravimetric and electrochemical study, **J. Ind Eng Chem,** 33 (2016) 288–297.
18. N. S. Victoria, R. Prasad, R. Manivannan, Psidium guajava leaf extract as green corrosion inhibitor for mild steel in phosphoric acid, **Int J Electrochem Sci**. 10(2015) 2220–2238.
19. R. Velayutham, K. Devarayan, G. Mayakrishnan, Corrosion inhibition of Eleusine aegyptiaca and croton rottleri leaf extracts on cast iron surface in 1 M HCl medium, **Appl Surf Sci**. 314(2014) 537–545.
20. E. H. Naoual, F. Rabiaa, T. Mustapha, Alkaloids extract of retama monosperma (L.) Boiss. seeds used as novel eco-friendly inhibitor for carbon steel corrosion in 1 M HCl solution: electrochemical and surface studies, **Appl Surf Sci**. 357 (2015) 1294–1305.
21. K. S. Sanjay, P. Anjali, B. O. Ime, Potential of azadirachta indica as a green corrosion inhibitor against mild steel, aluminum, and tin: a review. **J Anal Sci Tech Tec**. 6(1) (2014) 1–16.
22. A. S. Fouda, S. H. Etaiw, W. Elnggar, Punica plant extract as green corrosion inhibitor for C-steel in hydrochloric acid solutions, **International Journal of Electrochemical Science**, 9(9) (2014) 4866-4883.
23. M. C. Elbouchtaoui, A. Anejjar, R. Salghi, M. Hmamouchi, B. Hammouti, Inhibition of steel corrosion in 1 M HCl by the essential oil of Thymuspallidus, **Der PharmaChemica**, 6(4)(2014) 406-414.
24. A. E. K. Benmenine, M. R. Ouahrani, N. Gherraf, M. L. Sekirifa, L. Baameur, Anticorrosive action study of retamaretam extracts on mild steel X 52 in 20 % H_2SO_4 solution, **Energy Procedia**, 50(2014) 401-405.
25. M. Sangeetha, S. Rajendran, J. Sathiyabama, A. Krishnaveni, Inhibition of corrosion of aluminium and its alloys by extracts of green inhibitors, **Portugaliae Electrochimica Acta**, 31(1) (2013) 41-52.
26. S. Leelavathi, R. Rajalakshmi, Dodonaeaviscosa (L.) leaves extract as acid corrosion inhibitor for mild steel - A Green approach, **Journal of Materials and Environmental Science**, 4(5) (2013) 625-638.
27. B. A. Abd-El-Nabey, A. H. Abdel-Gaber, A. Ali, M.E.S. Khamis, S. El-Housseiny, Inhibitive Action of cannabis plant extract on the corrosion of copper in 0.5 M H_2SO_4, **International Journal of Electrochemical Science**, 8(5) (2013) 7124-7137.
28. M. Faustin, A. Maciuk, P. Salvin, Corrosion inhibition of C38 steel by alkaloids extract of Geissospermum laeve in 1 M hydrochloric acid: electrochemical and phytochemical studies, **Corros Sci**. 92 (2015) 287–300.
29. C. Maxime, R. Florent, A. Nadine, Enhanced corrosion resistance of mild steel in 1 M hydrochloric acid solution by alkaloids extract from Aniba rosaeodora plant: electrochemical, phytochemical and XPS studies, **Electrochim Acta** 131 (2014) 96–105.
30. A, Xavier, S. Stango and U. Vijayalakshmi, Studies on corrosion inhibitory effect and adsorption behavior of waste materials on mild steel in acidic medium, **Journal of Asian Ceramic Societies**, 6(1) (2018) 20-29, DOI: 10.1080/21870764.2018.1439608.